Inst. Phys. Conf. Ser. No 138: Section 5
Paper presented at the Electron Microscopy and Analysis Group Conf. EMAG93, Liverpool, 1993

The characterisation of delta-doping in gallium arsenide by Fresnel contrast

R E Dunin-Borkowski*, D D Perovic†, Z R Wasilewski‡ and W M Stobbs*

* Dept.of Mat. Sci. and Met., Pembroke Street, Cambridge CB2 3QZ
† Dept. of Met. and Mat. Sci., University of Toronto, Toronto, Ontario, M5S 1A4, Canada
‡ Inst. for Microstructural Sciences, NRC of Canada, Ottawa, K1A 0R6, Canada

ABSTRACT: A silicon delta-doped layer in gallium arsenide is characterised using TEM Fresnel contrast and regression analysis of HREM images. Surprisingly, the doped layer exhibits a *higher* scattering potential than the surrounding GaAs. It is shown that this is explained by the observed higher than expected rigid body contraction across the layer.

1. INTRODUCTION

Concentrated sheets of dopant atoms can be grown in semiconductors to act as quasi 2D electron gas systems. Such 'delta' doping needs to be well characterised to model electronic properties. For B in Si it has recently been shown that this can be done using the Fresnel Method in the TEM (e.g. Ross and Stobbs (1991a)) for nominally δ-doped layers at concentrations of less than 1at% (Dunin-Borkowski et al., 1993), despite the effects of absorption for this system. Here we apply the same approach to the characterisation of δ-doping in GaAs. It is generally considered that such layers can be more localised than in Si, however the GaAs:Si system is difficult to assess by the Fresnel approach, because of the small predicted change in scattering potential associated with substitutional incorporation of the dopant. A further complication is that, whereas in *bulk* GaAs silicon atoms are expected to dope n-type up to a concentration of ~0.01at% and increasingly amphoterically thereafter (Neave et al. 1983), what happens for *delta-dop*ing at high concentrations is unclear.

2. RESULTS OF FRESNEL METHOD APPRAISAL OF SILICON δ-DOPING

A test structure was grown in {001} GaAs, consisting nominally of a series of δ-doped layers of increasing concentration spaced 50nm apart. A low growth temperature of 500°C was used in order to preserve the narrow width of the δ layers at even their highest concentrations. The specified structure is shown in Fig.1a - the maximum nominal sheet concentration in the top layer is $3.2 \times 10^{13} cm^{-2}$ (5.1at%), which gives a *decrease* in scattering potential relative to GaAs of $\Delta V = 0.14V$ assuming no change in the GaAs lattice parameter. The Fresnel series examined comprised 11 plates and was taken using a Philips CM30 and an objective aperture of semi-angle 3.8mrad (Airy disc radius 0.60nm). The beam convergence was 0.33mrad and the crystal was orientated on the 001 systematic row 4.7° from {100}. Accurate defoci were fitted to the images using power spectra from the contamination at the specimen edge, and the defocus step size between images was calculated to be 684nm. Particular care was taken experimentally to maintain a low contamination level (which causes background phase contrast noise). Accordingly it was decided to use cleaved wedge specimens, of known specimen thickness profile, given their limited contamination (with the disadvantage that the specimen thickness increases rapidly). An accelerating voltage of 100kV was also used to minimise knock-on damage. Atomistic multislice simulations were computed to simulate the

© 1993 IOP Publishing Ltd

experimental image series using consistent parameters, with C_S=2.0mm, a focal spread of 29nm and image sampling at 0.01 nm/pixel. Neutral atom scattering factors, which are likely to be more realistic than ionic values if the doping is indeed amphoteric, were used.

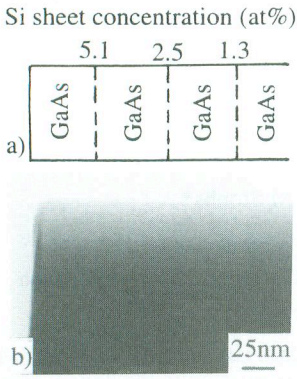

Fig.1 a) Nominal structure b) One image from the series at defocus -3229nm

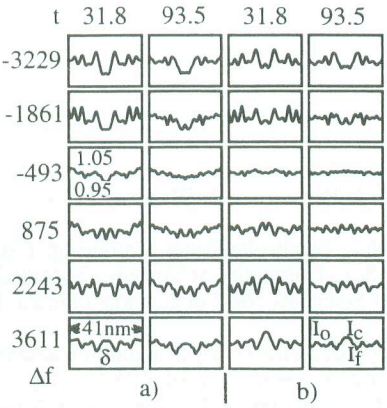

Fig.2 Digitised fringe profiles at the defoci Δf and thicknesses t shown (nm) a) before & b) after dividing by the in-focus image.

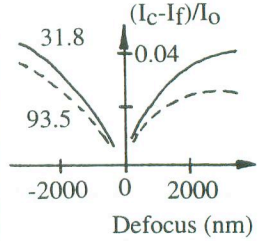

Fig.3 Experimental 1st fringe contrast vs Δf for the profiles of Fig.2b at the specimen thickness shown (nm).

An image from the experimental series (with the layering vertical) is shown in Fig.1b. Note that, despite the fact that the contrast has been digitally enhanced, only the Si layer with the highest concentration is visible. This layer was chosen for analysis at regions with mean specimen thicknesses of 32 and 94nm (determined accurately from the geometry of the 90° wedge), as indicated in Fig.1b. Each plate was digitised and the images were scaled to provide absolute electron intensities. The rapidly varying thickness limited the profiling projection length, used to minimise random noise contributions, to 15nm. This corresponds to a 31nm range in specimen thickness! Hence, the signal to noise ratio achieved was low. For a weakly diffracting orientation, as used here, we can ignore any asymmetry in the profiles when measuring an average profile and 'symmetrised' versions of the contrast were used for assessing the doping profile. Fig.2a shows the layer profiles for the two specimen thicknesses after removing the highest frequency noise and symmetrising. Slight absorption (differential scattering out of the objective aperture) is visible at zero defocus. Given the smaller ionic radius of Si (0.117nm) relative to that of both Ga (0.126nm) and As (0.118nm), the increased absorption at the doped layer is probably related to diffuse scattering associated with locally varying elastic displacements around misfitting dopant atoms. Such effects cause the *bright* contrast exhibited by B layers in Si in high angle annular dark field images (e.g. Perovic et al., 1991). Ross and Stobbs (1991b) have shown that small levels of absorption can be dealt with successfully by dividing the entire series by the in-focus profile. This approach yields the more familiar form of Fresnel contrast evident in Fig.2b. Neglecting the small contrast features originating from the processing, we can compare the more gross experimental and theoretical central fringe contrast as defined in Fig.2b. The major feature in the experimental profiles is that the contrast shows a bright central fringe overfocus and a dark central fringe underfocus. This indicates a layer of *increased* scattering potential (though that of Si is lower than that of both Ga and As!). However, the contrast depends on the mean forward scattering potential V_o and this is affected by both the composition and the lattice spacing of the layer. Graphs of the experimental fringe contrast (after removal of absorption) are shown in Fig.3 for the profiles in Fig.2b and exhibit contrast changes with defocus characteristic of a diffuse layer. The contrast is about a factor of four lower than for Si:B.

The effect on Fresnel fringe contrast of substitutional Si doping in GaAs is demonstrated by the simulations in Fig.4, which are for 5% Si confined to a single Ga layer, with no change in the GaAs lattice parameter. The contrast, as expected, is indicative of a region of lower scattering potential and is opposite in sense to that seen experimentally. The effects on the

contrast of both composition and expected lattice contraction (as scaled via the ionic radii and the atomic fraction of dopant) can be predicted from the graphs in Fig.5a. The experimentally observed contrast is indicative of a layer with a higher V_0 than that of GaAs. However, it is clear from Fig.5a that Si *lowers* the scattering potential of GaAs when it dopes substitutionally, *whichever* site it substitutes for. For the lattice contraction predicted using ionic radii, only substitution onto predominantly Ga sites raises the scattering potential above that of GaAs, and even then minimally. Fig.5b shows the predicted rigid body displacement (rbd) across such δ layers . For 5% δ-doping, the maximum rbd of only 0.0016nm is again associated with substitution for Ga atoms only. While a significant concentration of interstitial atoms could be responsible for an increase in V_0, this would be associated both with a lattice expansion and much more absorption than is observed. We therefore assume here that the doping is purely substitutional.

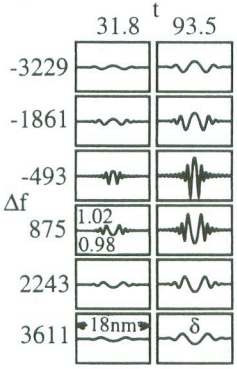

Fig.4 Simulations at Δf and t shown (nm) for 5% Si in one layer and no contraction.

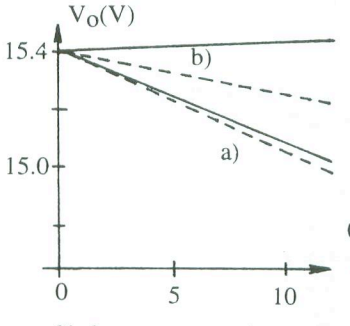

Fig.5 Predicted Vo vs at% Si a) no contraction, b) prediction from ionic radii, ——Si on Ga sites only,– –amphoteric doping

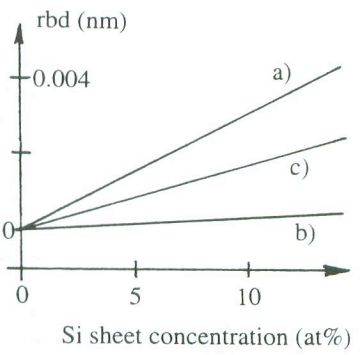

Fig.6 Predicted rbd vs at% Si from ionic radii for doping on a) Ga, b) As and c) Ga & As sites

It is now clear that an interpretation of the Fresnel contrast due to the silicon relies on a knowledge of the true rbd across the layer. The regression analysis technique of Stobbs, Wood and Smith (1986) (based on on an accurate determination of lattice fringe positions at identical specimen thicknesses on either side of an interface) can be used to determine such a rbd to an accuracy of about 0.002nm. Accordingly 004 lattice fringe positions across the δ layers (in JEOL 4000EXII images) were plotted vs fringe number, after removing variations in fringe spacing due to distortions from the microscope and densitometer lenses. It can be seen from Fig.7 (showing the rbd vs number of fringes used as a function of the starting fringe number, for the layer containing nominally 2.5% Si) that the value the rbd tends to stabilises as the size of the region analysed is increased. The three δ layers with the highest concentrations were analysed and their measured rbds are shown in Fig.8. Given that the layers were grown to have compositions varying by a constant factor, their rbds should (to first order) vary linearly. This is apparent from Fig.8, which includes a measurement from a section of pure GaAs. We can thus have confidence in the otherwise surprising result that the measured contraction for the 5% Si layer is about 0.01nm, and thus roughly six times larger than the value predicted from the ionic radii on a simplistic atomic fraction based ratio!

We can now examine the effect on the simulated Fresnel contrast of a rbd as large as this. For comparison Fig.9 shows simulations for 5% Si confined to a single Ga layer using the value for the rbd predicted from ionic radii. The contrast is very low indeed, the density change caused by the rbd compensating for the difference in scattering factor between Si and Ga. In contrast, simulations (Fig.10) including the experimentally determined rbd (but now with Si realistically spread amphoterically over five Ga and As atomic layers) show a clear bright central fringe overfocus and a dark fringe underfocus, as seen experimentally. Fig.11 shows the contrast vs defocus graph for this model, together with the experimental contrast. The

simulations are now approaching a realistic match with the experimental data for high defoci, and it should be noted that the high predicted contrast at low defoci is indicative of the need to smooth and broaden still further the composition profile (see Ross and Stobbs (1991a).

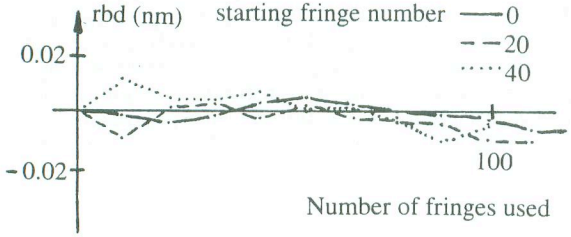

Fig.7 Measured rbd vs number of fringes used as a function of the indicated starting fringe number from the interlayer position, for the nominally 2.5at% Si δ layer.

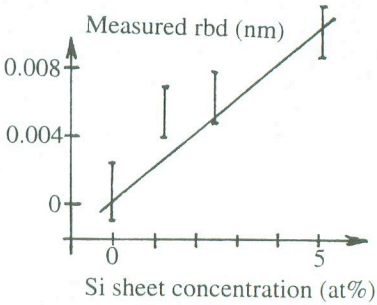

Fig.8 Measured rbd vs nominal silicon concentration.

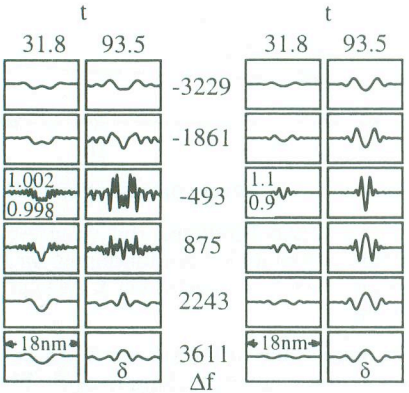

Fig.9 Simulation: 0.0016nm rbd; Si on one Ga layer

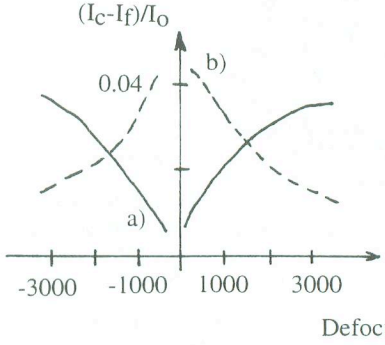

Fig.10 Simulation: 0.01nm rbd; Si on five Ga/ As layers

Fig.11 First fringe contrast: a) Experiment, b) 0.01nm rbd with Si spread over five Ga/ As layers

In summary, it has been shown that the Si δ layer examined exhibits a surprisingly higher scattering potential than GaAs. The consistency of our modelled analysis for this observation indicates that the lattice has contracted across the layer much more than would be simplistically predicted. This suggests that strong Si-As bonding can distort the lattice more than would otherwise be expected for layered doping and a high atomic fraction of Si on Ga sites.

It is a pleasure to thank Dr. CJD Hetherington for the high resolution work and for preparing specimens, Prof. CJ Humphreys for laboratory facilities and GEC for financial support.

REFERENCES

RE Dunin-Borkowski, WM Stobbs and DD Perovic 1993 *Microscopy of Semiconducting Materials, Oxford*, in press
JH Neave, PJ Dobson, JJ Harris, P Dawson and BA Joyce 1983 *Appl. Phys.* **A32**, 195
DD Perovic, GC Weatherly, RF Egerton, DC Houghton and TE Jackman 1991 *Phil. Mag.* **A63**, 757
FM Ross and WM Stobbs 1991a *Phil. Mag.* **A63**, 37
FM Ross and WM Stobbs 1991b *Ultramicr.* **36**, 331
WM Stobbs GJ Wood and DJ Smith 1986 *Ultramicr.* 14 145